Journal of Solid Mechanics Vol. 9, No. 4 (2017) pp. 794-801

Mechanical Characteristics and Failure Mechanism of Nano-Single Crystal Aluminum Based on Molecular Dynamics Simulations: Strain Rate and Temperature Effects

R. Rezaei[1] , H. Tavakoli-Anbaran[2], M. Shariati [3,*]

[1]*Faculty of Mechanical Engineering, Shahrood University of Technology, Shahrood, Iran*
[2]*Faculty of Physics, Shahrood University of Technology, Shahrood, Iran*
[3]*Department of Mechanical Engineering, Faculty of Engineering, Ferdowsi University of Mashhad, Mashhad, Iran*

Received 20 July 2017; accepted 24 September 2017

ABSTRACT

Besides experimental methods, numerical simulations bring benefits and great opportunities to characterize and predict mechanical behaviors of materials especially at nanoscale. In this study, a nano-single crystal aluminum (Al) as a typical face centered cubic (FCC) metal was modeled based on molecular dynamics (MD) method and by applying tensile and compressive strain loadings its mechanical behaviors were investigated. Embedded atom method (EAM) was employed to represent the interatomic potential of the system described by a canonical ensemble. Stress-strain curves and mechanical properties including modulus of elasticity, Poisson's ratio, and yield strength were determined. Furthermore, the effects of strain rate and system temperature on mechanical behavior were obtained. It was found that the mechanical properties exhibited a considerable dependency to temperature, but they hardly changed with increase of strain rate. Moreover, nucleation and propagation of dislocations along the plane of maximum shearing stress were the mechanisms of the nanocrystalline Al plastic deformation.

Keywords: Nanocrystalline aluminum; Mechanical properties; Molecular dynamics; Defromation mechanism.

1 INTRODUCTION

ADVANCES in nanotechnology have enabled development of nanodevices for a wide range of applications [1]. Metals, semiconductors, and insulators are widely used as three basic materials in production of nanoelectromechanical systems (NEMS), which integrate electrical and mechanical functionalities of a class of nano-devices such as sensors, actuators, gears, cantilevers, and accelerometers [2, 3]. Understanding properties of metallic materials at atomic scale based on experimental and/or numerical methods are therefore required to characterize and produce these new emerging nanostructured devices. Aluminum (Al) as the second most widely used metal has a great importance due to its specific structural properties. Furthermore, FCC metals, especially Al, as materials used in production of nanoscale devices and nano-composite materials, it is required to study and

*Corresponding author. Tel.: +98 511 880 5159; Fax: +98 511 880 6055.
E-mail address: mshariati44@um.ac.ir (M. Shariati).

analyze their mechanical properties at atomistic level [1]. Classical molecular dynamics (MD), as a reliable and powerful simulation technique at atomistic level [4], has been widely used by a number of researchers to model and simulate the elastic-plastic deformation mechanisms of metallic materials subjected to different loading conditions [5-9]. The authors have successfully utilized MD simulations to study the mechanical characteristics and deformation mechanisms of nanomaterials and nanocomposites in their previously published work [10-13]. Lim and Zhong simulated an Al slab with an Al (110) surface for bulk and surface analyses by using MD [14]. Khan et al. [15] studied the bulk mechanical properties of nanocrystalline Al obtained by consolidating powders of different grain sizes under compression. Their results demonstrated that the nanocrystalline Al was sensitive to strain rate and reduction in grain size resulted in increase in hardness and strength. Groh et al. [16] presented a multiscale materials modeling approach to predict the deformation response of an aluminum single crystal under compression. Yuan et al. [17] simulated the tension behavior of nano-single crystal Al under different temperatures by employing MD method. They utilized the Morse potential for defining the interaction potential energy between atoms. Their results showed the employment of Morse potential is able to render elastic, plastic and fracture behaviors for the model crystal and the tensile strength decreased at higher temperature. Li et al. [18] studied the surface energies of Al with different miller indices with an analytic long-range interaction embedded atom potential. Hachiya and Ito [19] presented a procedure for deriving an angular-dependent semi-empirical hybridized nearly-free-electron-tight-binding-bond potential to be used for MD simulations for Al and its compounds. Alavi and Thompson [20] performed MD simulations to determine the melting points of aluminum nanoparticles of 55-1000 atoms with Streitz-Mintmire variable-charge electrostatic plus potential. Ozgen and Duruk [21] modeled Al by using Sutton-Chen potential including many body interactions. They reproduced amorphous and crystal structures of aluminum by applying fast cooling and slow cooling treatments, respectively, by means of MD simulations, and examined the structural properties. Gao and Zhang [22] investigated FCC crystalline plasticity under an extremely strain rate by using a new dislocation-mechanics-based constitutive model. Guo et al. investigated the size and strain rate effects of the mechanical responses of single crystal copper under shear loading by MD simulations [23]. They showed that the yield stress decreases with the specimen size and increases with the strain rate. Karimzadeh et al. [24] investigated the nano-indentation test on Al using finite element method. They obtained Young's modulus and hardness by performing tensile and indentation tests, respectively. Literature review shows that the influences of temperature and strain rate on the mechanics of nanocrystalline Al and its fracture mechanism have not been under investigation experimentally or numerically at nanoscale level for uniaxial tensile and compressive loads using EAM potential.

In this study, the tensile and compressive behaviors of single crystal Al were thus investigated based on MD simulations. EAM potential was used to describe the interatomic energy of the system. The effects of temperature and strain rate in a wide range on elastic-plastic deformations, stiffness, strength, and failure of the system were studied by employing mechanical compressive and tensile tests. Stress-strain curves, mechanical properties including elastic modulus, Poisson's ratio, and yield strength were obtained. Then, the deformation mechanism and dislocation nucleation inside the material were explained using the obtained simulation results.

2 POTENTIAL FUNCTION AND SIMULATION SETUP

MD is a method for simulating thermodynamic behavior in three phases of solid, liquid and gas by using force, position and velocity of particles [21]. Among these agents, force is the most important. In classic MD simulation, force is derived from spacial derivative of potential function which describes the interactions between particles. Main purpose in MD simulation is the calculation of macroscopic behavior of the system by using a microscopic model. This model includes the mechanical interactions between the particles. Statistical mechanics provides an appropriate theoretical tool for performing MD simulation [25]. Embedded atom method (EAM), which was introduced by Daw and Baskes [26], is a multi-body potential function which was used in this study to describe the interactions among Al particles. The total potential energy of the system in the EAM framework is composed of a pairwise sum of interactions between atoms and a sum of embedding functions of atoms:

$$U_{total} = \sum_{i=1}^{N-1} \sum_{j=i+1}^{N} \varphi(r_{ij}) + \sum_{i=1}^{N} F(\rho_i) \tag{1}$$

$$\rho_i = \sum_{i=1}^{N-1} \psi(r_{ij}) \tag{2}$$

where the subscripts i and j indicate the unique pairs of atoms among the N atoms of the system, r_{ij} is their separation distance, $\varphi(r_{ij})$ is the pairwise interatomic energy, and $F(\rho_i)$ stands for the embedding potential function for atom i which depends on the total electron density, ρ_i , experienced by that atom.

In order to model and simulate nano-single crystal Al, a simulation specimen was created in according to face centered cubic structure (fcc) of Al material for carrying out the tensile and compressive tests, as shown in Fig. 1. This model was consisted of 6 unit cells in the y and z directions and 20 unit cells along x direction. The x-, y-, and z-axes were positioned perpendicular to the crystalline planes (100), (010), and (001), respectively. This specimen was composed of 3120 Al atoms and the value of its lattice constant was set to 0.405 *nm* [27].

Boundary conditions of the specimen were assumed periodic in x- and z-directions and free in y-direction. The initial velocities of the Al atoms in thermodynamic equilibrium with temperature T were assigned based on a Gaussian distribution function with a mean of 0.0. A Nose-Hoover temperature thermostat was employed to control the system temperature. An NPT ensemble was utilized for the equilibrium process and an NVT ensemble for the mechanical tests. Pressure was taken zero for NPT ensemble. Before doing the mechanical tests, the system was relaxed by running the model for 10000 time steps. The molecular dynamics simulator LAMMPS (Large-Scale Atomic/Molecular Massively Parallel Simulator) was utilized to conduct the mechanical tests [28]. EAM parameters and their corresponding values provided by Mendelev et al. [29] were adopted in LAMMPS to determine the interactions of the specimen particles.

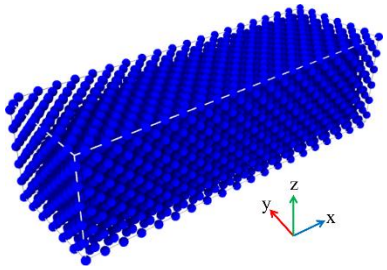

Fig.1
Initial configuration of the simulation specimen with the crystalline planes (100), (010), and (001) along x-, y-, and z-axes, respectively.

3 SIMULATION RESULTS AND DISCUSSION

The simulation time steps were set to 0.005 *ps* for the reduced temperatures equal to and higher than $T_r = 0.3$ and to 0.001 *ps* for the lower temperatures. This is because that the system for low temperature especially close to absolute zero was unstable for large time steps. The reason of this can be attributed to the motion of the atoms with higher frequencies at these temperatures. Reduced temperature, T_r , is defined as the temperature ratio of the system, T , to the melting point, T_m , of bulk aluminum, that is, $T_r = T/T_m$. The Al melting point was assumed $T_m = 933.6K$. After relaxation of the system, the tensile strain load $\dot{\varepsilon} = 10^9 s^{-1}$ was applied to the specimen and stretched in x-direction at the temperature $T = 300K$. Then, the specimen was subjected to a compressive strain load of the same rate. The stress-strain curves of the material and its mechanical properties were calculated. Table 1. shows the obtained values for Young's modulus, E , Poisson's ratio, v , and yield strength, σ_y , along with those previously reported in literature for the purpose of comparison. The elastic moduli and Poisson's ratios were in good agreement with those of experimental bulk Al. This indicates the behavior consistency of the nano-model with the experimental bulk material in the elastic regime. The compressive Young's modulus was somewhat higher than the tensile one, while the strength at tensile loading was much higher than that of compressive condition. The numerical yield stresses obtained in this work and also those reported in the literature was much higher than the experimental results for bulk aluminum. It can be contributed to this fact that the constructed numerical models are perfect and no defect or impurity are embedded in it. Indeed the miniaturization of materials from macroscales or microscales to

the scales of several nanometers leads to severe changes in the mechanical properties. Such observations have been made for many nanomaterials that have been studied over the past decades [30].

Table 1
Mechanical properties of nano-single crystal Al in comparison with the other reported results.

	Method	Test	$E\,(GPa)$	v	σ_y (GPa)
Present work	MD	Tension	63.2	0.39	4.13
		Compression	65.6	0.36	2.96
Ref. [31]	MD	Tension	79.8	--	6.0
Ref. [17]	MD	Tension	--	--	2.3
Ref. [24]	FEM	Tension	75.3	--	150 (*MPa*)
		Nanoindentation	79.8	--	203 (*MPa*)
Ref. [32]	Bulk Al	Experiment	70	0.35	100 (*MPa*)

3.1 Effects of strain rate

In order to investigate the effects of strain rate on mechanical characteristics of nano crystal aluminum, the constructed specimen was subjected to tensile and compressive conditions by applying strain loads of different rates, i.e. $\dot{\varepsilon} = 10^7, 10^8, 10^9$ and $10^{10} s^{-1}$. Then the elastic modulus, E, and Poisson's ratio, v, were calculated. Fig. 2(a),(b) shows the dependence of these quantities on strain rate for tension and compression loadings, respectively. As observed in this figure, the influences of the rate of strain loads were negligible. The Young's modulus and also Poisson's ratio remained nearly constant by changing the velocities of the external loadings. It was also observed that the yield strength of the material was almost independent of the strain rate, as depicted in Fig. 3, except that a small different trend was seen for the highest strain rate $\dot{\varepsilon} = 10^{10} s^{-1}$. The same trend was observed for yield strain of the sample as a function of strain rate, as shown in Table 2. The results illustrated a small deviation at dependence of yield stress and strain for the highest strain rate.

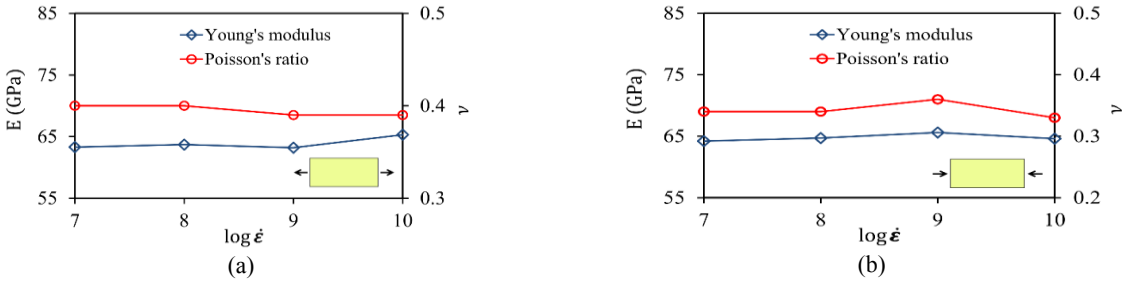

Fig.2
Effects of strain rate on Young's modulus and Poisson's ratio of nano crystal Al.

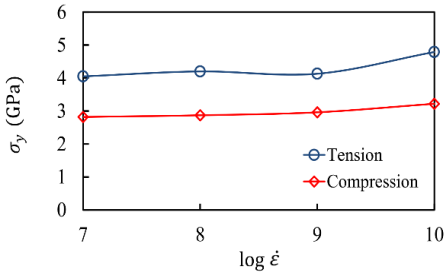

Fig.3
Effects of strain rate on yield strength of nano crystal Al for tension and compression tests.

Table 2
Effects of strain rate on the yield strain of nano crystal Al for tensile and compressive loadings.

$\dot{\varepsilon}$	10^7	10^8	10^9	10^{10}
Tension	0.084	0.085	0.086	0.105
Compression	0.043	0.045	0.046	0.052

3.2 Effects of temperature

To examine the effects of temperature, the tension and compression tests were again acted on the specimen for different values of temperature. In each test, the temperature was controlled by a thermostat in the applied NVT ensemble and the mechanical properties were then calculated from the data obtained from the simulations. The obtained results including Young's modulus and Poisson's ratio are illustrated in Fig. 4(a),(b) as a function of reduced temperature from $T_r = 0.01$ to 0.9 for tension and compression, respectively. As shown in Fig. 4, Young's modulus considerably decreased by increasing temperature from the room temperature ($T_r = 0.32$) to the melting point, and it increased by bringing down the test temperature to absolute zero. While Poisson's ratio went down by decreasing the temperature to zero and it went up by increasing the temperature from the room temperature for both loading conditions. In brief, the simulation results reported significant influences of temperature on the mechanical behavior of nano-single crystal Al.

The yield strengths of the specimen are plotted in Fig. 5 as a function of reduced temperature for both applied tensile and compressive loadings. As observed in this figure, the strength of the sample decreased extremely by increasing the temperature from $T_r = 0.01$ to 0.9 for both loading conditions. Another point is that the compressive yield strength was lower than the tensile one for all the temperature. Table 3. shows the dependence of yield strains to the system temperature. The yield strain significantly decreased by increasing the temperature. Also, the material yielded at smaller strain for compression loading.

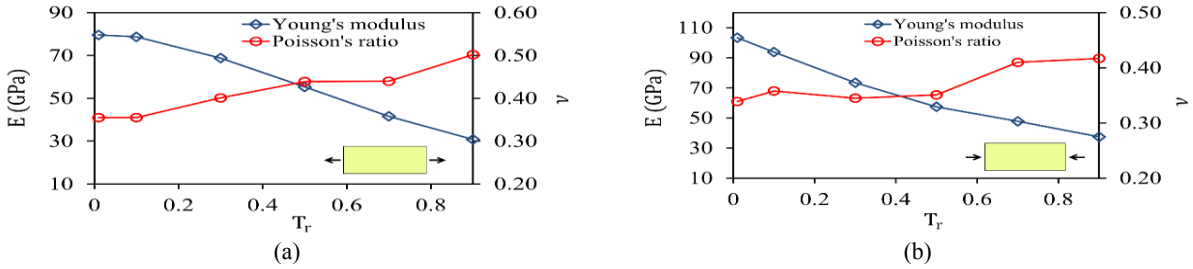

Fig.4
Effects of temperature on Young's modulus and Poisson's ratio of nano crystal Al for tension (a) and compression (b) tests.

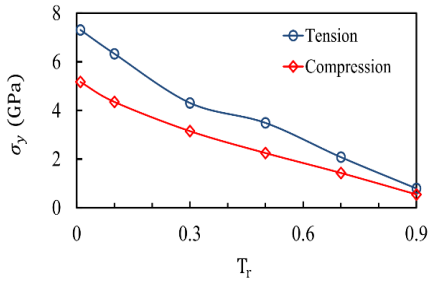

Fig.5
Influence of temperature on yield strength of nano crystal Al for tensile and compressive loadings.

Table 3
Effects of temperature on the yield strain of nano crystal Al for tensile and compressive loadings.

T_r	0.01	0.1	0.3	0.5	0.7	0.9
Tension	0.114	0.106	0.085	0.086	0.073	0.05
Compression	0.061	0.053	0.048	0.048	0.032	0.028

3.3 Deformation mechanism

Fig. 6 shows the stress-strain curves of the tensile and compressive failures of the specimen under applied strain loadings. The boundary conditions along the *x*- and *y*-axes were periodic and it was free along the *z*-axis which allowed the system to be deformed in this direction under the employed strain loads. As shown in Fig. 6(a),(b), the influences of the strain rates $\dot{\varepsilon} = 10^7, 10^8, 10^9$ and $10^{10} s^{-1}$, on the tensile and compressive behaviors of the specimen were not considerable, except that a small difference was seen for the high strain rate $\dot{\varepsilon} = 10^{10}$. The specimen was elastically stretched or compressed then by reaching the yield strength, it plastically deformed via nucleation and propagation of the dislocation of the particles as shown in Fig. 6. The first peak of these curves indicate the yield point of the material and also the first nucleation and propagation of the dislocation inside the material.

Other pick points in the plastic regions of the stress-strain curves and the following sudden drops of the stresses indicates the nucleation and propagations of the atoms under the external applied tension and compression loads. The following raising stresses after each pick point in the plastic region prove the resistance of the material against the next nucleation and propagation.

The effects of the system temperature from $T_r = 0.01$ to 0.9 on the deformation mechanism are plotted in Fig. 6(c),(d), respectively, for the uniaxial tension and compression tests for the strain load $\dot{\varepsilon} = 10^9$. The obtained results showed an extreme dependency of the metal elastic-plastic deformations to temperature. By increasing the temperature, the extent of the elastic region was decreased and therefore the plastic deformation was occurred at a lower applied strain.

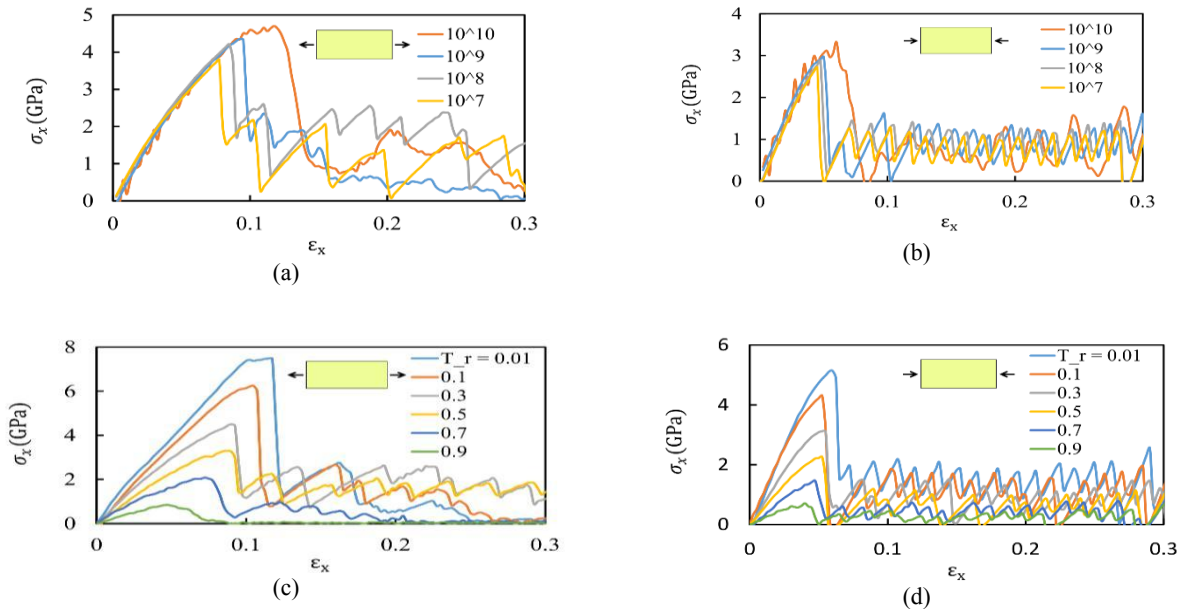

Fig.6
Stress-strain curves of nano crystal Al and effects of strain rate (a,b) and temperature (c,d) for tension (a,c) and compression (b,d) tests.

Fig. 7 shows the deformation mechanism of the specimen for both tension (on left column) and compression (on right column) at the room temperature $T = 300K$ and for the applied strain rate $\dot{\varepsilon} = 10^9$. In each part of this figure, the top and bottom images indicates the deformation mechanism and its corresponding colored shearing strain field, respectively. Figs. 7(a) and (d) show the elastically deformed specimen just before yielding point for the tension and compression, respectively. Also, Figs. 7(b) and (e) show the deformed specimen just after the yielding point for the tension and compression, respectively. The top inset in the middle of Fig. 7 illustrates the deformation mechanism for the tensile stretching of the specimen in more details. As shown in this inset, the dislocation of the atoms along the slip plane was the reason of the yielding and therefore the plastic deformation of the metal. In addition, stretching and dislocation resulted in appearing necking in the transverse direction from the free surface as shown in the top inset of Fig. 7. The bottom inset in Fig. 7 shows the deformation mechanism of the metal under the compression test. Dislocation and propagation were also the mechanism of deformation in the specimen along the

slip planes under the external applied load. For both uniaxial loading conditions the dislocation was observed along the plane of maximum shearing stress and also the crystalline plane (101). Then the deformation concentrated in the neck region and finally the ductile fracture was occurred along the maximum shearing planes as shown in Figs. 7(c),(f).

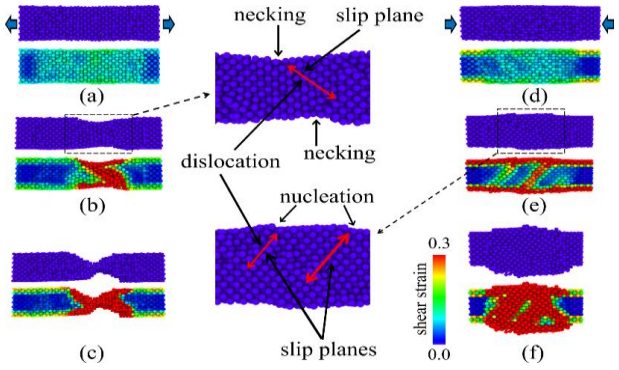

Fig.7
Deformation mechanism of nano crystal Al for $T = 300K$ and $\dot{\varepsilon} = 10^9$: (a,d) specimen elastically stretched or compressed before yielding, (b,e) dislocation of the particles during plastic deformation, (c,f) failure mechanism of the specimen along the plane of maximum shearing stress, respectively, for the tensile and compressive loadings.

4 CONCLUSIONS

In this study, MD simulations were employed to investigate the influence of strain rate and temperature on the mechanics of nanocrystalline Al as a typical FCC metal. The stress-strain curves and the mechanism of the plastic deformation were obtained. EAM potential was used to describe the interatomic energy of the system. In brief, the following conclusion remarks can be drawn for FCC nanocrystalline metals based on the obtained results:

a. The mechanical behavior of Al were predicted by the applied EAM potential parameters for both uniaxial tensile and compressive loading conditions.
b. The strain rate did not demonstrate considerable effects on the mechanical properties and elastic-plastic deformation of the material for both tension and compression.
c. The temperature had significant effects on the deformation mechanism and mechanical characteristics of the specimen for both tests.
d. The nucleation and propagation of dislocation of the particles were the mechanism of material deformation and failure. Slip planes were observed along the plane of maximum shearing strain for both tensile and compressive strain loads. Ductility of nano metal stemmed from the dislocation nucleated from the free surface.

The obtained results in the present work revealed more the characteristics of nanocrystalline FCC metals and also their dependency degrees to temperature and externally applied compressive and tensile loading rates. In addition, this study went into detail about the mechanisms of nanoplasticity.

REFERENCES

[1] Bhushan B., 2004, *Springer Handbook of Nanotechnology*, Spinger-Verlag Berlin Heidelberg.
[2] Dao D. V., Nakamura K., Bui T. T., Sugiyama S., 2010, Micro/nano-mechanical sensors and actuators based on SOI-MEMS technology, *Advances in Natural Sciences: Nanoscience and Nanotechnology* **1**(1):013001-013010.
[3] Ekinci K. L., Roukes M. L., 2005, Nanoelectromechanical systems, *Review of Scientific Instruments* **76**: 061101.
[4] Rapaport D., 2004, *The Art of Molecular Dynamics Simulation*, Cambridge University Press.
[5] Narayan K., Behdinan K., Fawaz Z., 2007, An engineering-oriented embedded-atom-method potential fitting procedure for pure fcc and bcc metals, *Journal of Materials Processing Technology* **182**: 387-397.
[6] Nath S. K. D., 2014, Elastic, elastic–plastic properties of Ag, Cu and Ni nanowires by the bending test using molecular dynamics simulations, *Computational Materials Science* **87**: 138-144.
[7] Ikeda H., Qi Y., Cagin T., Samwer K., Johnson W. L., Goddard W. A., 1999, Strain rate induced amorphization in metallic nanowires, *Physical Review Letters* **82**: 2900.
[8] Koh S. J. A., Lee H. P., 2006, Molecular dynamics simulations of size and strain rate dependent mechanical response of FCC metallic nanowires, *Nanotechnology* **17**: 3451-3467.

[9] Wu H. A., 2004, Molecular dynamics simulation of loading rate and surface effects on the elastic bending behavior of metal nanorod, *Computational Materials Science* **31**: 287-291.
[10] Rezaei R., Shariati M., Tavakoli-Anbaran H., Deng C., 2016, Mechanical characteristics of CNT-reinforced metallic glass nanocomposites by molecular dynamics simulations, *Computational Materials Science* **119**: 19-26.
[11] Rezaei R., Deng C., 2017, Pseudoelasticity and shape memory effects in cylindrical FCC metal nanowires, *Acta Materialia* **132**: 49-56.
[12] Rezaei R., Deng C., Shariati M., Tavakoli-Anbaran H., 2017,The ductility and toughness improvement in metallic glass through the dual effects of graphene interfae, *Journal of Materials Research* **32**: 392-403.
[13] Rezaei R., Deng C., Tavakoli-Anbaran H., Shariati M., 2016, Deformation-twinning mediated pseudoelasticity in metal-graphene nanolaminates, *Philosophical Magazine Letter* **96**: 322-329.
[14] Lim M. C. G., Zhong Z. W., 2009, Molecular dynamics analyses of an Al (110) surface, *Physica A* **388**: 4083-4090.
[15] Khan A., Suh Y. S., Chen X., Takacs L., Zhang H., 2006, Nanocrystalline aluminum and iron: Mechanical behavior at quasi-static and high strain rates, and constitutive modeling, *International Journal of Plasticity* **22**: 195-209.
[16] Groh S., Marin E. B., Horstemeyer M. F., Zbib H. M., 2009, Multiscale modeling of the plasticity in an aluminum single crystal, *International Journal of Plasticity* **25**: 1456-1473.
[17] Yuan L., Shan D., Guo B., 2007, Molecular dynamics simulation of tensile deformation of nano-single crystal aluminum, *Journal of Materials Processing Technology* **184**: 1-5.
[18] Li R., Zhong Y., Huang C., Tao X., Ouyang Y., 2013, Surface energy and surface self-diffusion of Al calculated by embedded atom method, *Physica B* **422**: 51-55.
[19] Hachiya K., Ito Y., 2002, Transition-metal-like interatomic potentials for aluminium, *Journal of Alloys and Compounds* **337**: 53-57.
[20] Alavi S., Thompson D., 2006, Molecular dynamics simulations of the melting of aluminum nanoparticles, *Journal of Physical Chemistry A* **110**: 1518-1523.
[21] Ozgen S., Duruk E., 2004, Molecular dynamics simulation of solidification kinetics of aluminium using Sutton–Chen version of EAM, *Materials Letters* **58**: 1071-1075.
[22] Gao C. Y., Zhang L. C., 2012, Constitutive modelling of plasticity of fcc metals under extremely high strain rates, *International Journal of Plasticity* **32-33**: 121-133.
[23] Guo Y., Zhuang Z., Li X. Y., Chen Z., 2007, An investigation of the combined size and rate effects on the mechanical responses of FCC metals, *International Journal of Solids and Structures* **44**: 1180-1195.
[24] Karimzadeh A., Ayatollahi M. R., Alizadeh M., 2014, Finite element simulation of nano-indentation experiment on aluminum 1100, *Computational Materials Science* **81**: 595-600.
[25] Field M. J., 2007, *A Practical Introduction to the Simulation of Molecular Systems*, Cambridge University Press.
[26] Daw M. S., Baskes M. I., 1984, Embedded-atom method: derivation and application to impurities, surfaces, and other defects in metals, *Physics Review B* **29**: 6443-6453.
[27] Callister W. D., Rethwisch D. G., 2011, *Fundamentals of Materials Science and Engineering: an Integrated Approach*, John Wiley & Sons.
[28] Plimpton S., 1995, Fast parallel algorithms for short-range molecular dynamics, *Journal of Computational Physics* **117**: 1-19.
[29] Mendelev M. I., Srolovitz D. J., Ackland G. J., Han S., 2005, Effect of Fe segregation on the migration of a non-symmetric sigma-5 tilt grain boundary in Al, *Journal of Materials Research* **20**: 208-218.
[30] Buehler M. J. ,2008, *Atomistic Modeling of Materials Failure*, Springer.
[31] Song H. Y., Zha X. W., 2010, Influence of nickel coating on the interfacial bonding characteristics of carbon nanotube–aluminum composites, *Computational Materials Science* **49**: 899-903.
[32] Beer F. P., Johnston E. R., Dewolf J. T., 2006, *Mechanics of Materials*, McGraw Hill.